EVOLUTION OF THE BROADLY RIFTED ZONE IN SOUTHERN ETHIOPIA THROUGH GRAVITATIONAL COLLAPSE OF DYNAMIC TOPOGRAPHY

By

LUELSEGED MENGESHA EMISHAW

Bachelor of Science in Geology

Addis Ababa University

Addis Ababa, Ethiopia

2012

Submitted to the Faculty of the
Graduate College of the
Oklahoma State University
in partial fulfillment of
the requirements for
the Degree of
MASTER OF SCIENCE
December, 2015

EVOLUTION OF THE BROADLY RIFTED ZONE IN SOUTHERN ETHIOPIA

THROUGH GRAVITATIONAL COLLAPSE OF DYNAMIC TOPOGRAPY

Thesis Approved:

Dr. Daniel A. Laó-Dávila

Thesis Adviser

Dr. Mohamed G. Abdelsalam

Dr. Estella A. Atekwana

ACKNOWLEDGEMENTS

I would like to thank my family for their loving guidance and help. The kindness and the love they show me fill my heart with hope and strength every day; you are always near and dear to my heart my beloved family, thank you.

This manuscript could not be finalized without the continuous and tireless support of Dr. Daniel A. Laó-Dávila, Dr. Mohamed G. Abdelsalam, and Dr. Estella A. Atekwana. And I would like to say that your help is greatly appreciated. Also, a many thanks to Dr. Stephen S. Gao for providing us with the seismic shear tomography study of the Main Ethiopian and Afar Rifts.

In addition, I would like to thank Boone Pickens School of Geology, Oklahoma State University and Statoil for the opportunity they have given me to advance my studies.

Finally, I would like to thank Dr. Gezaygn Yirgu, Dr. Balemual Atnafu, Mr. Adrian Hell, Mr. Luke Swift, Dr. Mohamed Abdelsalam, and members of the Tectonic Research Group. The way I see the science of geology has been greatly influenced by these people.

Name: LUELSEGED MENGESHA EMISHAW

Date of Degree: DECEMBER, 2015

Title of Study: EVOLUTION OF THE BROADLY RIFTED ZONE IN SOUTHERN ETHIOPIA THROUGH GRAVITATIONAL COLLAPSE OF DYNAMIC TOPOGRAPY

Major Field: GEOLOGY

Abstract: The Broadly Rifted Zone (BRZ) is a 300 km wide diffused zone of extension in southern Ethiopia that connects the narrow (50-65 km wide) South Main Ethiopian Rift and the Eastern Branch of the East African Rift System (EARS) represented by the Kenya and Turkana rifts. The topographic features of the BRZ resemble those of the Basin-and-Range in the western United States in that they are characterized by the presence of NE-trending ridges and valleys superimposed on regionally uplifted (~2 km average elevation) terrain. This rift morphology, which is unique to the BRZ within the EARS, resulted from the presence of tilted blocks of Eocene-Pliocene volcanic rocks bounded by steep normal faults that exhibit half-grabens geometry. The tilted blocks rest unconformably on Precambrian crystalline basement and the half-grabens are filled with Miocene-Pliocene sedimentary rocks. The geodynamic mechanism through which the BRZ was developed is not well understood. Previous studies proposed that the BRZ hosts both tectonically active and inactive rift basins resulting from northward propagation of the Kenyan Rift and southward propagation of the Southern Main Ethiopian Rift. In order to understand the relationship between crustal and upper mantle structures beneath the BRZ and its unique morphological expression and extensional style, we first estimated the Moho depths using two-dimensional (2D) radially-averaged power spectral analysis of the World Gravity Map (WGM 2012) satellite gravity data. Subsequently, to verify results from the 2D radially averaged power spectral analysis, we developed lithospheric-scale 2D forward models along E-W profiles across the BRZ and extensional structures to north and south of it. We found that the Moho topography depicts a dome shape beneath the BRZ and it shallows to a minimum depth of 27 km in the central part of this dome. We suggest that the Moho doming, topographic uplift and arching of the crust underlying the BRZ is the result of mantle upwelling beneath the BRZ from a deeper asthenospheric source that changed to northeast lateral flow at shallower depth. This is supported by results from seismic tomography results which show the presence of low velocity anomaly of shear wave at lithospheric depth of 0-100 km and 100-175 km stretching in a NE-direction from beneath the BRZ to the Afar Depression. At depths between 175-250 km and 250-325 km the low shear wave velocity anomaly became only a broad elliptical feature centered beneath the BRZ. This created gravitationally unstable dynamic topography that triggered extensional collapse leading to the formation of the BRZ as a wide rift within the narrow rift system of the EARS.

TABLE OF CONTENTS

LIST OF FIGURES

CHAPTER 1

INTRODUCTION

Extension of the continental lithosphere creates rift basins that vary in their geometry and morphological expression that is influenced by the structure of the pre-rift crust and the sub-continental lithospheric mantle, presence of thermal anomalies at various lithospheric levels and the different levels of stretching factors and strain rate (Alen and Alen, 2005; Armitage and Allen, 2010). Two contrasting types of these rift basins are referred to as narrow continental rifts and supra-detachment rift basins (also referred to as wide continental rifts). Narrow rifts are best exemplified by the majority of the segments of the East African Rift System (EARS) that are less than 100 km in width (Figure 1A). Narrow continental rifts generally develop within relatively thick, cold and strong lithosphere where the localization of the extensional strain is facilitated by the presence of mechanical and/or thermal weaknesses such as inherited Precambrian structures and intrusion of magmatic bodies (Ebinger and Casey, 2001; Chorowicz, 2005). These rifts are typically underlain by thinned crust and sub-continental lithospheric mantle where thinning is restricted to a narrow and linear zone that follows the surface expression of the rift basin. Differently, wide continental rifts such as the Basin and Range of the western United States are wider than 100 km and develop within thin, hot, and weak lithosphere (e.g. Pancha et al., 2006; Goldsworthy et al., 2002).

These rifts are underlain by a crust that is heterogeneously thinned from a previously thickened continental crust (Wernicke et al., 2000). The wide rifts are also underlain, at least in parts, by broad zones of thin sub-continental lithospheric mantle (e.g. Schulte-Pelkum et al., 2011). The thinning of broad sections of the sub-continental lithospheric mantle beneath the wide rifts has been explained as due subducted slab detachment or due to sub-continental lithospheric mantle delamination (e.g. Wells and Hoisch, 2008).

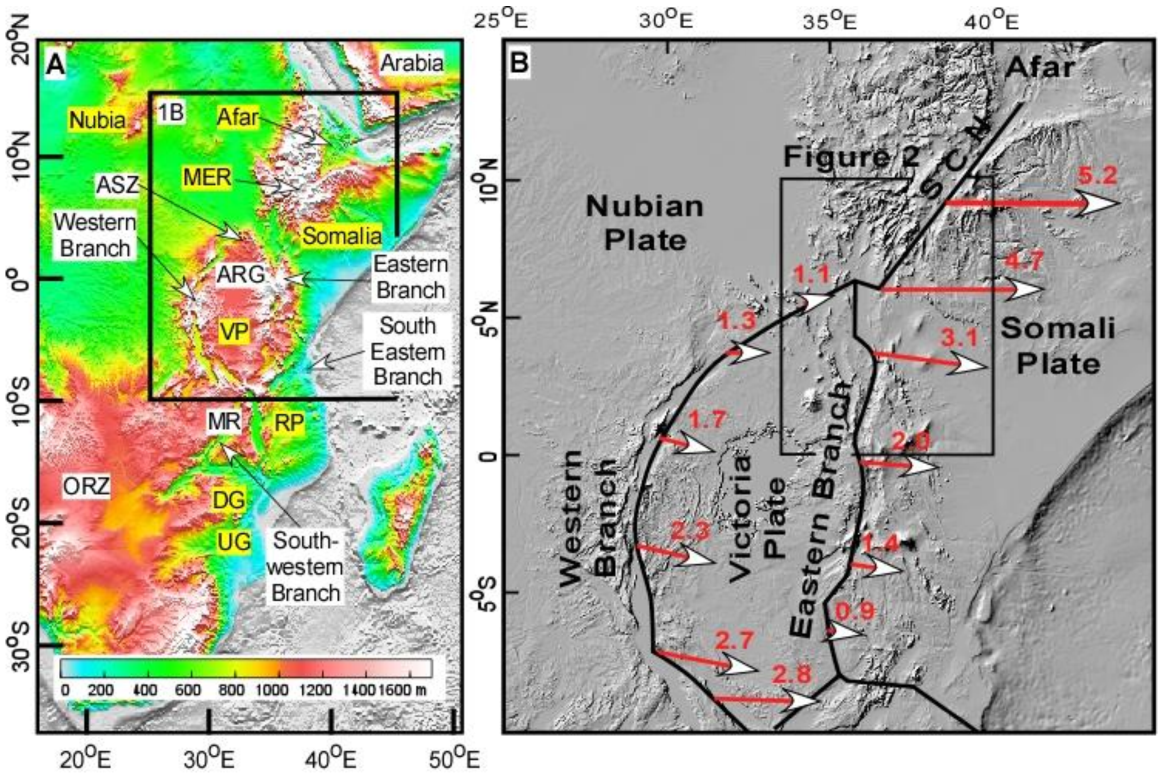

Figure 1. Map showing the tectonic setting of the EARS. (A) A color hillshade map showing the Northern, Eastern, South-eastern, Western, and South-western Branches of the EARS. (B) The SRTM-DEM map showing the relative motions of the Somalia and Victoria plates in mm/yr. Saria et al., (2014). The black box shows the area of the Broadly Rifted Zone and the Eastern and Northern Branches of the EARS.

The surface and upper crustal structures of narrow rifts are dominated by the presence of curvilinear and high-angle border faults that accommodate extension and control the subsidence in the basin during the early stages of rifting, often through the development of half-grabens with along-strike alternation and change of half-graben polarity (e.g. Ebinger and Casey, 2001). In contrast, wide continental rifts are characterized by the presence of both high-angle (rider faults) and low-angle normal detachment faults, which account for the accommodation of the extension that can reach 250% as in the case of the Basin and Range (e.g. Wernicke, 1981). Additionally, extension during the development of wide continental rifts can lead to the exhumation of the lower crust, hence the formation of metamorphic core complexes (e.g. Lister and Davis, 1989; Fritz et al., 1996; Arca et al., 2010).

The EARS (Figure 1A) is considered a classic example of a narrow continental rift, where most of its individual segments are 70-100 km wide and form asymmetric rift basins flanked by steep normal faults (Chorowicz, 2005). The northern part of the EARS stretches within Ethiopia, Eritrea and Djibouti and it constitutes the Afar Depression in the north and the Main Ethiopian Rift to the south (Figure 1B). The Main Ethiopian Rift in turn is divided into northern, central and southern segments (Figure 2; Abebe et al., 2007; Corti, 2009). Unlike any other segment of the EARS, the Southern Main Ethiopian Rift, which is ~80 km wide broadens into a 300 km zone of diffused extension, which is referred as the Broadly Rifted Zone (BRZ) (Figure 2; Moore and Davidson, 1978; WoldeGabriel and Aronson, 1987; Ebinger et al., 2000; Philippon et al., 2014) and this zone sometimes also refer to as the Basin and Range of Ethiopia (Corti, 2009). South of the BRZ, the EARS extends as the Eastern Branch which is represented by the ~70 km wide Kenyan Rift (Figure 2; Ebinger et al., 2000).

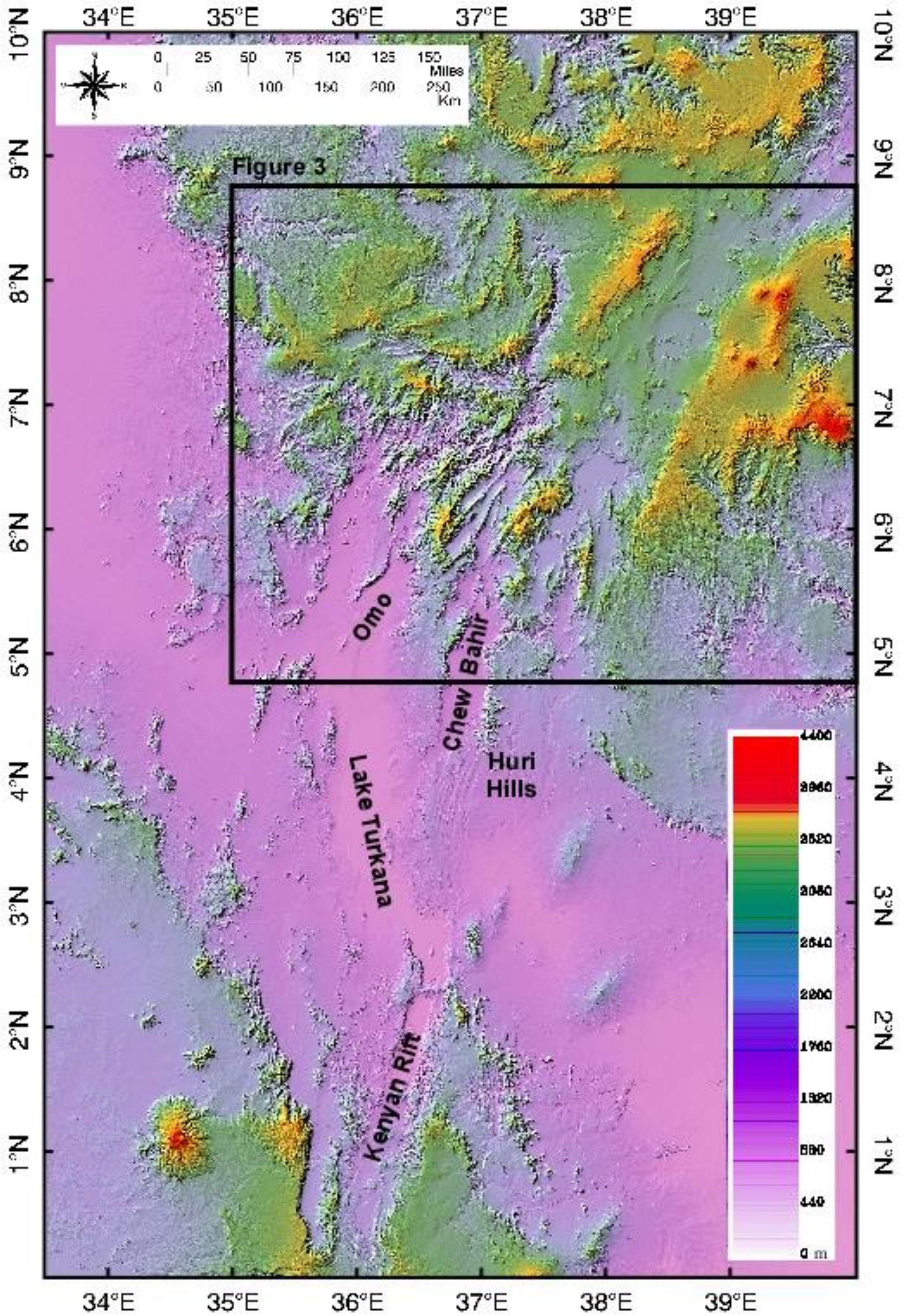

Figure 2. Map showing the topography of the Kenyan Rift, the SMER, and the BRZ from SRTM-DEM data. Black box encloses the area of the BRZ expanded in Figure 3.

The BRZ consists of 10-15 km wide basins that form a Basin-and-Range type topography (Figure 3) not observed anywhere else in the EARS (Moore and Davidson, 1978; Ebinger et al., 2000; Corti, 2009). This topography resulted from the presence of tilted blocks of Eocene-Pliocene volcanic rocks bounded by steep normal faults forming half-graben geometry. The tilted blocks rest unconformably on Precambrian crystalline basement and the half-grabens are filled with Miocene-Pliocene sedimentary rocks (Figure 4-6). Ebinger et al. (1993; 2001) suggested that the structural characteristics of the BRZ are typical of those of narrow rift basins. Additionally, although the Precambrian crystalline basement (typically gneisses and migmatites indicative of middle crustal level of metamorphism) is exposed in many places on the surface, no low-angle detachment faults or metamorphic core complexes are observed within the BRZ. These observations suggest that the BRZ developed through processes different from those suggested for other wide rifts such as the Basin and Range. Results from field, remote sensing, chronological, geomorphological, and kinematic studies were used to suggest that the BRZ is an overlap zone between the SMER and the Kenyan Rift (Figure 2; Ebinger et al., 2001). Further, the development of individual basins constituting the BRZ has been explained as the eastward migration and the northward propagation of Kenyan Rift, and the southward propagating of the SMER (Cerling and Powers, 1977; Moore and Davidson, 1978; W-Gabriel and Aronson, 1987; Ebinger et al., 2000; Bonini et al., 2005; Philippon et al., 2014). In addition, polyphase oblique rifting events have been proposed as a factor that might have influenced the width of the BRZ (Boccaletti et al., 1998; Corti, 2009; Bonini et al., 2005).

This study used two-dimensional (2D) radially-averaged power spectral analysis of the World Gravity Model (WGM2012) satellite data to image depths to the Moho beneath the BRZ and its surrounding. In addition, we developed 2D forward models from WGM2012 satellite gravity data to construct E-W trending lithospheric-scale cross-sections across the BRZ. The 2D forward models help to verify the Moho depth estimates from the 2D radially-averaged power spectral analysis and to compare lithospheric structure between the narrow rifts to the north and south with those of the BRZ.

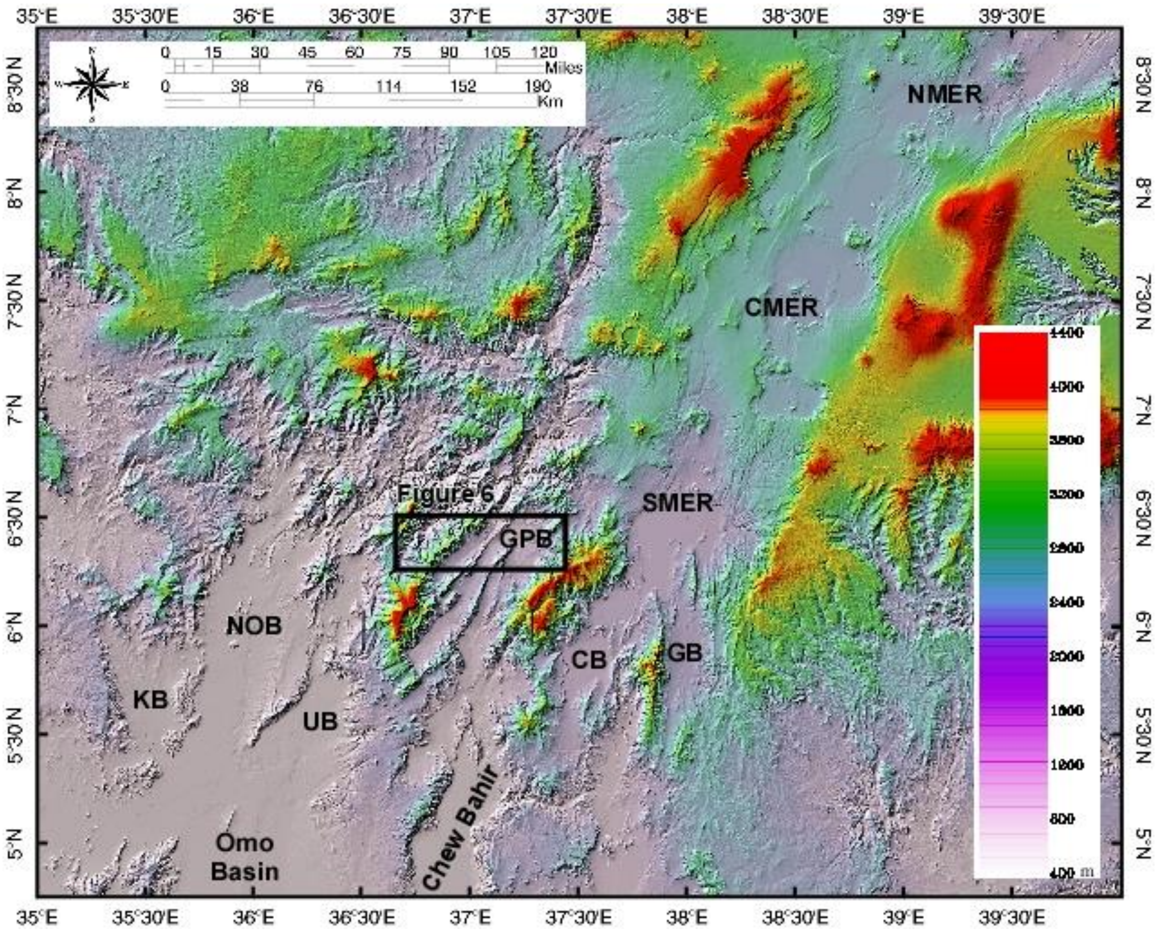

Figure 3. Map showing the topography of the BRZ from SRTM-DEM data. The topography resembles a Basin-and-Range type topography (Corti, 2009). The western, the central, and the eastern portions of the BRZ display distinct tectonic settings. The black box encloses the area of the Gofa Province Basins expanded in Figure 6.

This study also used horizontal density slicing of shear wave seismic tomography of Grand (2002) model at various depths to understand deeper lithospheric and asthenospheric structures beneath the BRZ. The aim of this work was to explore any relationship between the geometry of the BRZ and its surface topographic expression and deeper features including the Moho depth and deeper lithospheric and asthenospheric structures.

CHAPTER II

TECTONIC AND GEOLOGIC SETTING

II.I. Tectonic setting of the EARS

The EARS is a complex divergent plate boundary between the Nubian, Somalian, and Arabian plates in its northern part, and between the Nubian, Somalian, Victoria and Rovuma plates in the southern part (Fig. 1; Saria et al., 2014). The EARS can be divided into three main branches; the Northern Branch, which constitutes the Afar Depression and the Main Ethiopian Rift; the Eastern Branch which constitutes the Kenyan Rift and the Tanzanian Divergent Zone; and the Western Branch that extends from the Rhino-Albertine graben through the Kivu Graben, Tanganyika Rift, Rukwa Rift, Malawi Rift and Dombe and Urema graben (Figure 1A; Saria et al., 2014). It extends for several thousand kilometers from the Afar Depression in the north in Ethiopia, Eritrea and Djibouti, to the Dombe and Urema graben to the south in Mozambique (Chu and Gordon, 1999; Chorowicz, 2005). South of the Afar Depression where rifting is in the verge of transitioning to seafloor spreading (Bridges et al., 2012), the EARS continues as the Main Ethiopian Rift which constitutes a northern, central and southern segments (Figure 1B) all where rifting is assisted by magmatic injections (Ebinger and Casey, 2002).

South of the southern segment of the Main Ethiopian Rift the EARS continues further south into the BRZ, thfocus of this study. Further south, the EARS bifurcates into the Eastern and Western Branches (Figure 1).

The Northern Branch displays the highest angular velocity of the Somalian plate relative to the Nubian plate that decreases from 5 5.2 mm/yr in the north to 4.7 mm/yr to the south. (Figure 1A; Saria et al., 2014). In the Eastern Branch the angular velocity of the Somali plate relative to the Nubian plate decreases from 3.1 mm/yr in the north to 0.9 mm/year in the south. Differently, in the Western Branch the angular velocity of the Victoria plate relative to the Nubian plate increases from 1.1 mm/year in the north to 2.8 mm/year to the south (Figure 1B; Saria et al., 2014).

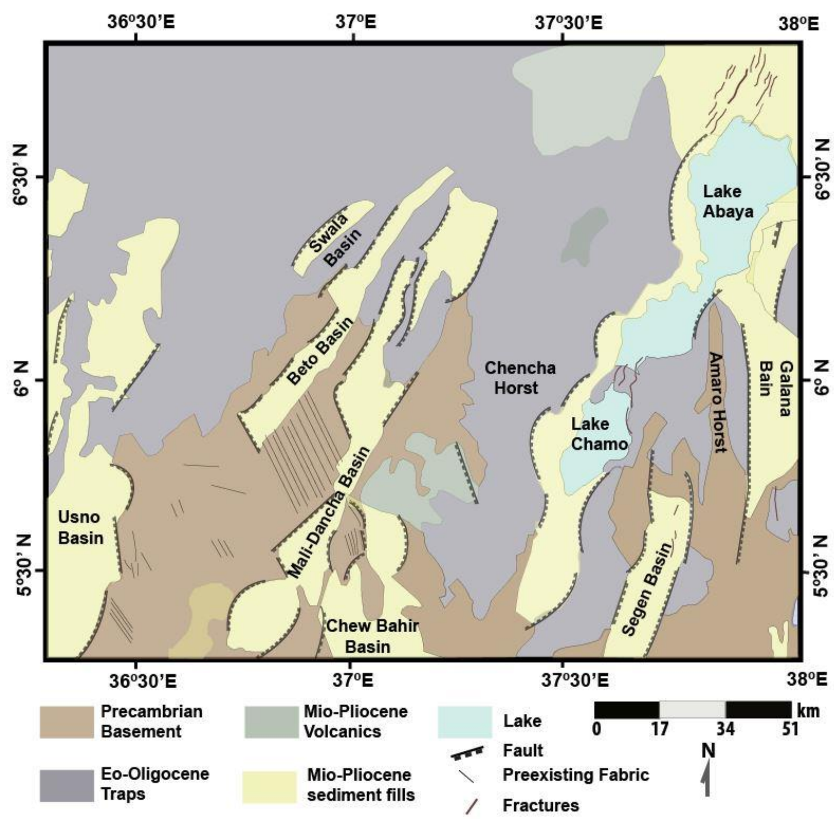

Figure 4. The geological map of the Gofa Province Basins, which shows the flood trap basalts, the basement and the sediment fills, after the geological map of Ethiopia (Mengesha et al., 1996). Fault and Precambrian fabric were mapped from SRTM DEM data at 90 m resolution.

The BRZ in the southern part of Ethiopia is considered as part of the Northern Branch of the EARS (Figures 3 and 3). The southern part of the southern segment of the Main Ethiopian Rift that strike N-S to NNE-SSW represents the eastern most basin of the BRZ and it bifurcates further south into the Chamo and Galana Basins (Figures 3-5). The Kenyan Rift extends northward into the Turkana Rift, which continues further north as the Omo Basin (Figure 2), Further north, the Omo Basin bifurcates into the Usno and the Northern Omo Basins, the latter represents the westernmost basin of the BRZ (Figures 3-5). The southern segment of the Main Ethiopia Rift and the Usno Basins enclose the Gofa Province, which represents the central and the north central part of the BRZ (Figure 3), The Gofa Province constitutes three 10-15 km wide half-grabens represented, from east to west, by the Mati Dancha, Bet and Swala Basins (Figure 6). The Mati Dancha Basin seems to extend southward as the Chew Bahir Basin (Figure 3). The half-graben of the Gofa Province have been formed by oblique rifting whereas the eastern (Galana Basin) and western (North Omo Basin) basins of the BRZ thought to be the result of the northward propagation of the Kenyan rift and the southward propagation of the southern segment of the Main Ethiopian Rift (Ebinger et al., 2000; Corti et al., 2009).

II.II. Evolution of the Broadly Rifted Zone

The BRZ is the region in which both the Northern Branch and Eastern Branch of the EARS interact. It consists of the southern segment of the Northern Branch represented by the southern Main Ethiopian Rift (Chamo and Galana Basins), the Gofa Province (Swala, Bet and Mati Dancha Basins), the Chew Bahir Basin, and the northern segment of the Eastern Branch represented by the Omo Basin (Usno and the Northern Omo Basins). This makes the width of the BRZ in an E-W direction 314 km. These basins are mainly bounded by steeply-dipping faults which have developed in early to middle Miocene (Ebinger et al., 1993; 2000). One of these basins in the central BRZ, the Chow Bahir Basin has serrated margins and 1,500 meters high steep escarpments (Figure 5F), and might be one of the several failed rifts (Moore and Davidson, 1978; WoldeGabriel and Aronson, 1987). Geochronological data from dikes on the flanks of the Chencha Horst north of Chew Bahir basin (Figure 3) as well as cosmogenic dating of fault escarpments suggest that extension in the southern segment of the Main Ethiopian Rift began around 20-21 Ma (Bonini et al., 2005; Pik et al., 2008).

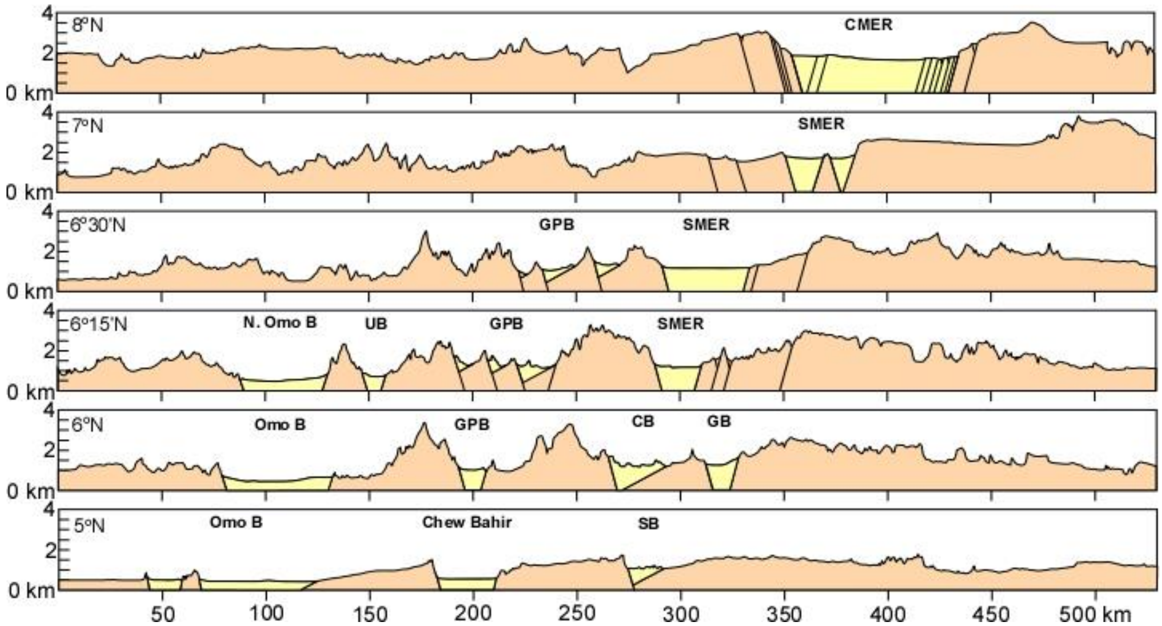

Figure 5. Cross sectional views of the BRZ at latitudes 8˚, 7˚, 6˚15', 6˚, and 5˚N. The cross sections show the northward and southward propagation and deflection of the Kenyan Rift and SMER, respectively. The cross section at latitude 6˚30' and 6˚15 N', Gofa Province Basins, displays a localized tectonic setting that does not directly interact with either the SMER or the Omo Rift.

The Kenyan Rift continues to the north into the Turkana Rift (Figure 2). The Turkana Rift comprises half-grabens bounded by mostly E-dipping planar and listric faults which dip between 22° and 60° (Dunkelman et al., 1988; Morley et al., 1992). The Kenyan Rift may have transferred the extension from west to east into the Turkana Rift in northern Kenya (Cerling and Powers, 1977; Morley et al., 1992; Ebinger et al., 2000).

Results of fault kinematic analyses conducted near the Chencha Horst (Figure 3) suggest four extensional events. The first extension was in a NNE-SSW direction and that was followed by an E-W direction as indicated by striae lineation superposed on the previous extensional structures (Bonini et al., 2005). The third phase of extension was in a NW-SE direction while the fourth and the last phase, which suggested to be Quaternary in age, was in an E-W direction (Bonini et al., 2005). However, focal mechanism fault plane solutions show dominant WNW-ESE directed regional extension (Ebinger, 2000), which is suggested be the result of clockwise rotation of the Somalian Plate relative to the Nubian Plate (Bonini et al., 2005). Boccaletti et al. (1998) suggested that oblique rifting causes transtensional structures such as pull apart rhomb-shaped basins.

II.III. The Role of Pre-existing structures in the evolution of the Broadly Rifted Zone

There are several opinions regarding the relationship between the BRZ and the Precambrian structures of the crystalline basement. For example, Boccaletti et al. (1998) suggested that localization of extensional strain might be facilitated by the reactivation of zones of pre-existing weaknesses. Ebinger et al. (2000however argued that there is little evidence for the reactivation of the low-angle gneissic foliations in the Precambrian crystalline basement throughout the development of the BRZ. However, Moore and Davidson (1987) observed that there is an apparent parallelism between the faults associated with the BRZ and the Precambrian metamorphic foliation and mylonite zones within the gneisses. Additionally, Moore and Davidson (1978) suggested that the arcuate pattern of the Gofa Province Basins and the serrated edge of the Chow Bahir Basin (Figure 3) might have resulted from the presence of regional variation in the trends of the Precambrian structures.

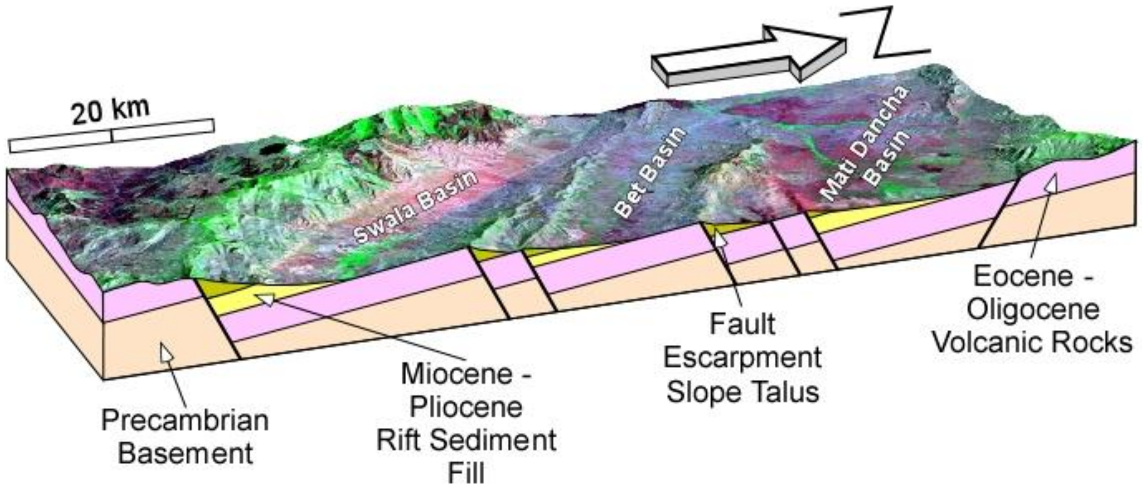

Figure 6. A 3D perspective view that shows the north-central portion of the BRZ, which is also called the Gofa Province Basin. The cross sectional view was constructed from a Landsat satellite image of 30 m spatial resolution. The Swala, Beto, and Mali-Dancha Basins make up the northern part of the BRZ.

II.IV. Current Models for explaining the Broadly Rifted Zone

Previous studies considered the breadth of the BRZ as the result of the interaction between the Kenyan Rift and the southern segment of the Main Ethiopian Rift. Moore and Davidson (1978) used the interpretation of aerial photographs to describe fault splays with an en échelon relationship at the southern termination of the southern segment of the Main Ethiopian Rift and the northern termination of the Kenyan Rift. Ebinger et al. (2000) concluded that the style of rifting is similar to that of narrower rift zones but distributed across a much broader region**.** The style of extensional structures, the presence of exhumed Precambrian basement rocks, and the presence of mantle plume related volcanism within the BRZ has been attributed to the mantle related lithospheric weakening and thinning (Ebinger et al., 2000; Bonini et al., 2005; Corti, 2009). This led to the suggestion that the anomalous width of the BRZ is the result from the south propagation of the southern segment of the Main Ethiopian Rift and the north propagation of the Kenyan Rift. The eastward migration of the Turkana Rift produced rift basins with an active eastward migration while the western rift basins that were aborted became failed rift basins (WoldeGabriel and Aronson, 1987; Ebinger et al., 2000; Bonini et al., 2005; Vétel and Le Gall, 2006; Corti, 2009). Bonini et al. (2005) further discussed the influence of the Somalian Plate clockwise rotational component on the development of the BRZ by causing the eastward transfer of the extensional strain.

CHAPTER III

DATA AND METHODS

III.I. World Gravity Model (WGM2012) satellite gravity data

We used World Gravity Model (WGM2012) satellite gravity data to map the Moho depths beneath the BRZ and its surrounding (Figure 7). The WGM2012 is a gravity anomaly map produced by combining the national Geospatial Intelligence Agency's Earth Gravity Model EGM2008, which incorporates gravity measurement of land, marine and gravity surveys, with Denmark's National Space Institute (DTU) 10 global field model and Earth Topographic 1 (ETOPO1) Global Relief model (Bonvalot et al., 2012).

The EGM2008 is a spherical harmonic model of Earth's gravitational potential. To develop EGM2008, the global set of area-mean free-air gravity anomalies, ITG-GRACE03S gravitational field model and associated covariance matrix were used. The global set of area-mean free-air gravity anomaly, which includes terrestrial, altimetry-derived and airborne gravity data, is defined on a 5 arc-minute equiangular grid. And the ITG-GRACE03S gravitational field models is designed by using a static high resolution model. WGM2012 is a combination of EGM2008, and the mean sea surface DTU10, and Earth Topographic elevation data of 1^{o} X 1^{o} ETOPO1 Global Relief Model (Palvis et al., 2012).

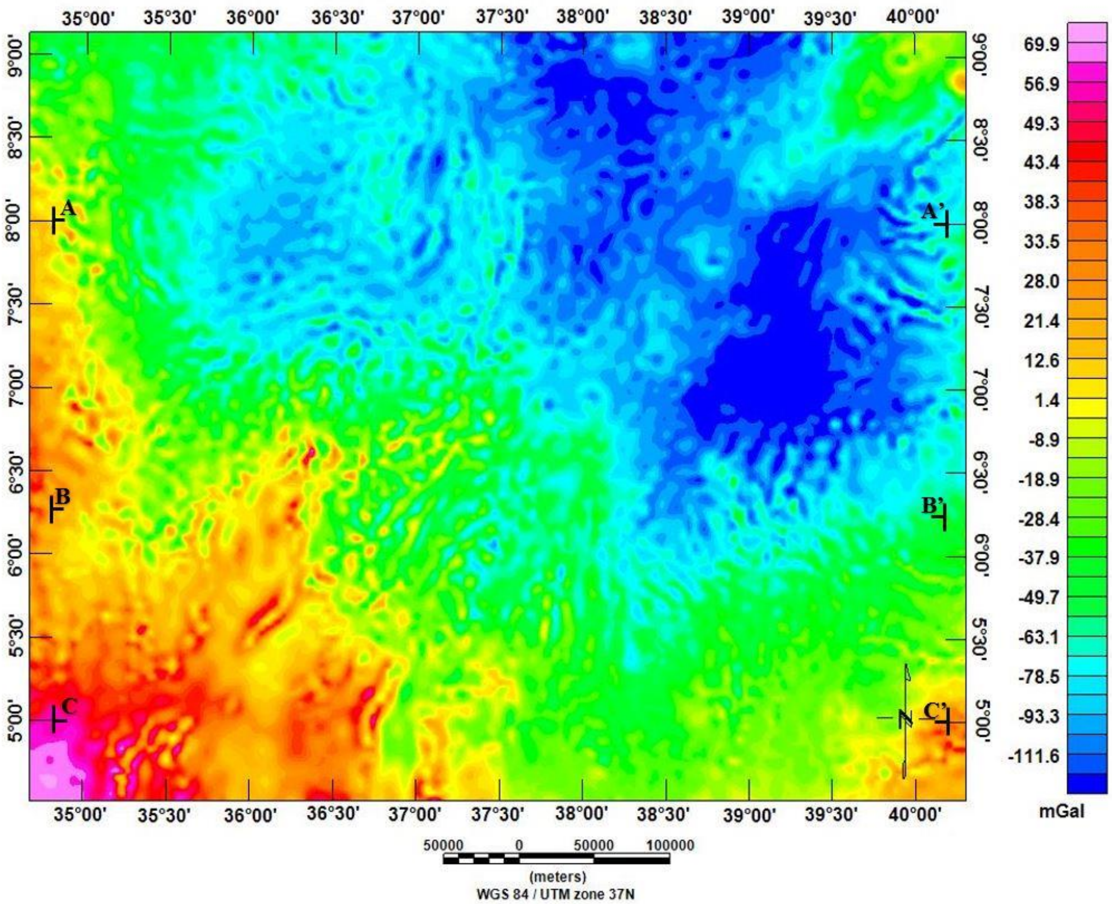

Figure 7. Map showing the Bouguer gravity anomaly of southern Ethiopia. The low gravity results are associated with rift basins while the higher values are associated with the presence of flood trap basalts in the area.

III.II. Two-dimensional (2D) Radially-averaged Power Spectrum Analysis

The spectral approach, a method employed onto the WGM-2012 satellite gravity data, has been successfully used to estimate the depths to the Moho of any observed ground, airborne or satellite gravity data. It relies on the principles of Fourier transformation in which an equal number of sinusoidal function-frequency domain can represent any functions in time or space domain. The power spectrum of a frequency domain is represented by:

$P_h(r) = e^{-2hr}P_0(r)$ (1)

where $P_h(r)$ is the power spectrum of the top gravity surface $P_0(r)$. The representation of this formula in linear equation,

$$\ln P_h(r) = -2hr + c \quad (2)$$ (where "h" is the slope (depth) and "c" is a constant);

results in the power spectrum graph from which the depth to the Moho can be estimated (Tselentis et al., 1988).

The 2D radially-averaged power spectral curves were computed from 1ºX1º windows (~110X110 km) of the WGM2012 gravity data covering the BRZ and surroundings with 50% N-S and E-W overlaps. Two hundred and twenty one spectral curves corresponding the 1ºX1º windows were produced covering an area of 316,350 km^2 within and around the BRZ. The Geosoft Oasis Montaj™ MagMap software was used to produce the 2D power-density spectral spreadsheet. The scatter plots of Ln-P vs. wavenumber were done in Excel. And the slope of the middle phase of the spectral curves were estimated by a LINEST equation, which is suited to estimate the slop of any exponential-linear curves. An example of the 2D radially-averaged power spectrum curve for a 1ºX1º window is shown in Figure 8.

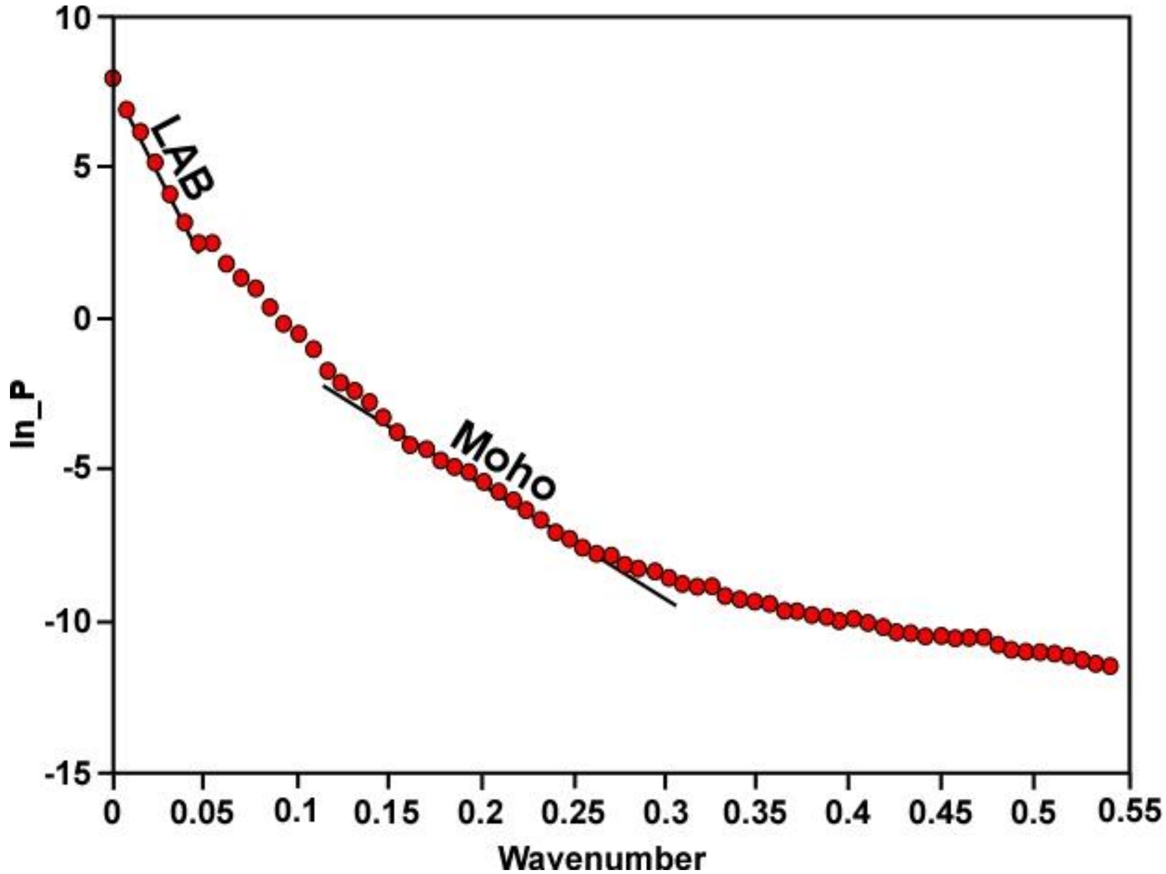

Figure 8. A 2D power-density spectral curve showing the wavenumber vs ln P (amplitude squared). The curves were computed from the WGM2012 gravity data of 1˚X 1˚windows (~ 110X100km). The Moho and the Lithosphere-Asthenosphere Boundary (LAB) depths (the slopes in black in the spectral curve) are computed by the LINEST equation, which determines the statistical fit of the slope curve against the original X-Y plot. This figure is given as an example to show how the 221 blocks for the Moho and 33 blocks for the LAB is calculated from 1˚X 1˚WGM2012 gravity satellite data. The LAB was calculated to see any pronounced anomaly beneath the Gofa Province Basins. Areas north and south of the Gofa Province Basins have not been considered. The slope in between the Moho and LAB possibly represents a certain discontinuity between the Moho and the LAB.

Similarly, we have used 1˚X 1˚windows of the WGM2012 gravity data to determine the Lithospheric Asthenosphere Boundary (LAB) of the southern Ethiopia. The slopes of the deeper source wavenumber values were calculated from the 2D radially-averaged power spectral curves. In so doing, wavenumber values that would negatively bias the would-be lithospheric thickness of a mobile belt were ignored.

III.III. Two-dimensional (2D) Forward Modeling

To verify Moho depth results obtained from the 2D radially-averaged power spectral analysis and to compare the cross-sectional view of the BRZ with extensional structures to the north and south of it, three 2D forward model models were constructed from the WGM2012 data. The models were constructed from the WGM2012 gravity dataset, which were extracted at 8^o N, 6^o 15’ N and 5^o N latitudes. And each profile extends from longitude 35^o E to 40^o E (Figure 7). These models are using the 2D GYMSYS Oasis Montaj software. The density values that were assigned for the upper crust, lower crust and the sub-continental lithospheric mantle are 2.6 gm/cm^{3,} 2.85 gm/cm^3 and 3.1 gm/cm^3, respectively. A value of 2.9 gm/cm^3 is also assigned for the partial melt of the sub-continental lithospheric mantle. The statistical fit of the observed profile against the calculated profile matches with an error of about 8%.

CHAPTER IV

RESULTS

IV.I. Results from the Two-dimensional (2D) Radially-averaged Power Spectrum Analysis

The Moho depth map of the BRZ and the surrounding (Figure 9A) shows a significant variation in the crustal thickness that ranges between 27 and 44 km. In order to compare the Moho depth variations with the surface morphological expression of the BRZ and its surrounding the transparent edition of the Moho depth map is draped onto a grey-scale hillshade DEM of the SRTM data (Figure 9B), which helps to illustrate both the Moho depth variation and surface morphology in a single image (Figure 9C). The central and the southern segments of the Main Ethiopian Rift along with the Ethiopian and Somalian plateaus show Moho depths greater than 35 km (Figure 9). On the other hand, the northern segment of Main Ethiopian Rift and the BRZ show Moho depths shallower than 35 km (Figure 9). The depth of the Moho beneath the Somalian Plateau ranges from 39 to 43 km and shows a relatively uniform crustal thickness. The Ethiopian Plateau shows a relatively shallower depths to the Moho (~ 37 km) that abruptly decrease to ~ 34 km from north to south along longitude 8° N. Also, along the longitude 8º 45’ N, the crustal thickness of the Ethiopian Plateau increases from ~ 35 km to ~ 37 km with an abrupt shift in thickness at about latitude 36º 15’ E. The Moho depths beneath the Main Ethiopian Rift show three distinct characteristic features for each of its three segments.

The Moho beneath the northern segment of the Main Ethiopian Rift is ~34 km in depth, and further deepens under the central segment of the Main Ethiopian Rift to ~38 km while the southern segment of the Main Ethiopian Rift show an elevated Moho of ~32 km in depth.

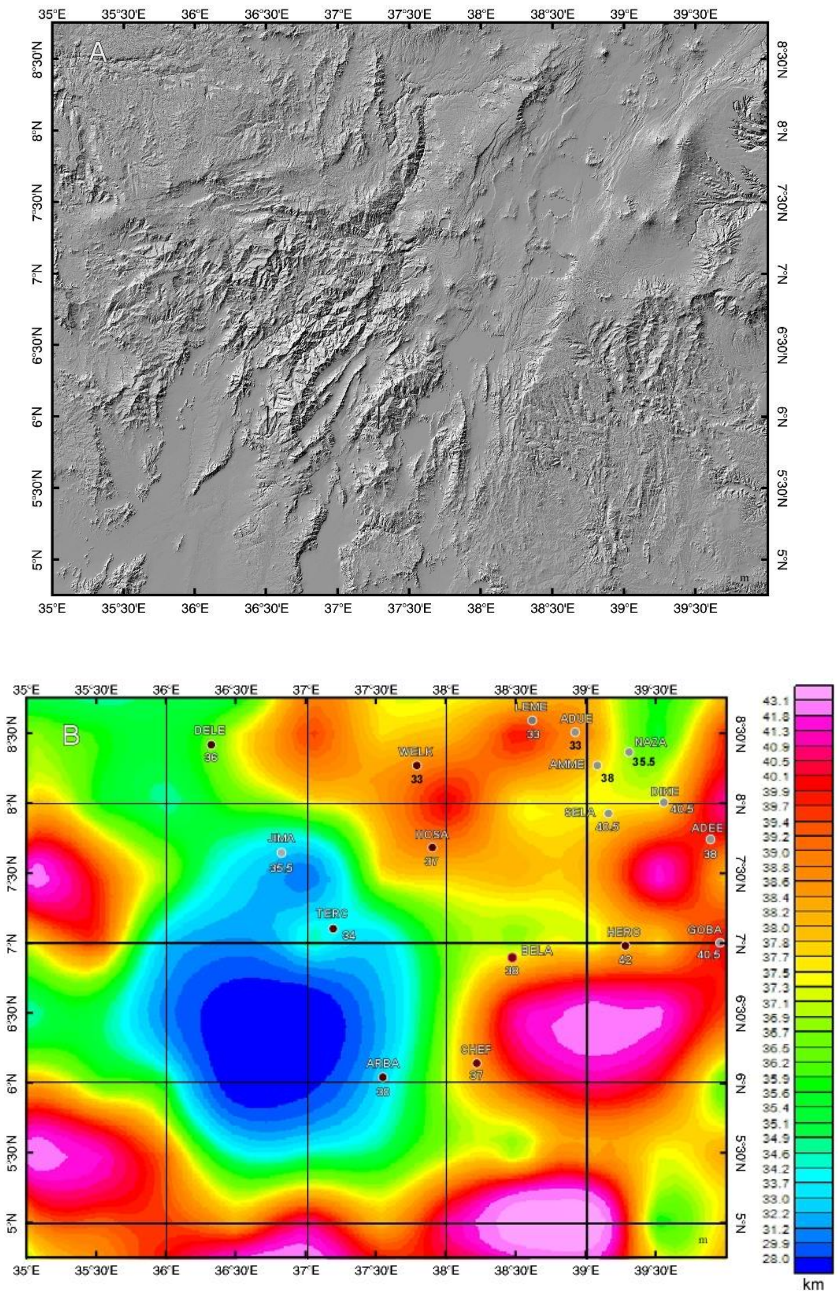

Figure 9C. Continued to page 30.

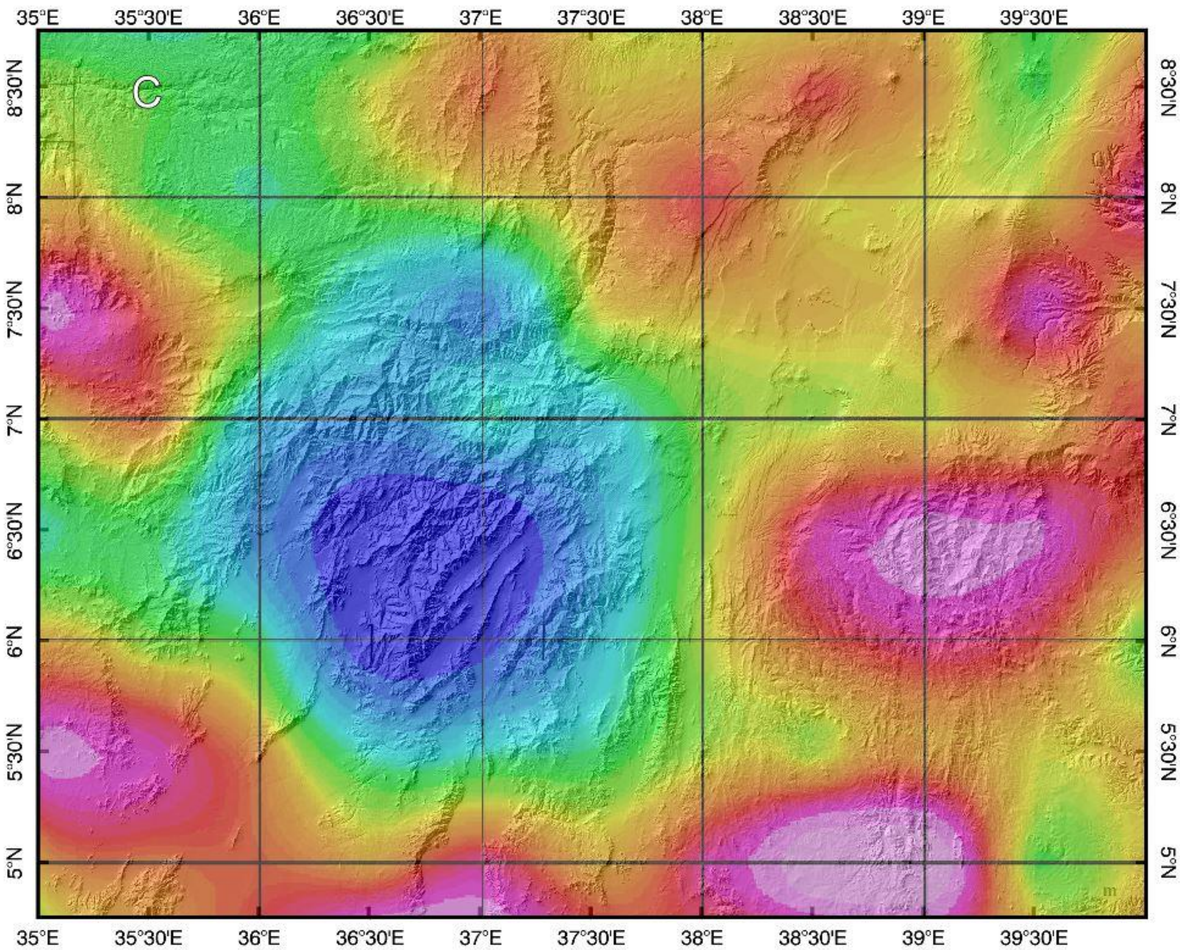

Figure 9. (A) Map showing an SRTM-DEM of the central and southern Ethiopia. (B) Map showing the Moho depths information for the region as in A. The elliptical feature in blue represents the shallower depths to the Moho while the pink represents the deeper depths. The Moho map was constructed from the Two-Dimensional (2D) spectral analysis of the WGM2012 gravity satellite data. The analysis was carried out in Geosoft Oasis Montaj^{TM} MagMap and Excel spreadsheet. Location points and data values in deep brown were taken from Dugda et al. (2005). Location points and data values in dark grey were taken from Keranen et al. (2009).

Beneath the Gofa Province Basins, the northern limit of the BRZ, the Moho depth gets shallower reaching a depth of ~27 km. There is a gradual Moho depth increase from the shallowest depths beneath the Gofa Province Basins to the deeper depth of 44 km, under the Ethiopian and Somalian plateaus. The shallow Moho anomaly forms a circular feature in the map view that is 210 km wide in the E-W direction and 240 km wide the N-S direction. The Moho is shallowest in the central part of this circular feature and becomes progressively relatively deeper away from the center suggesting that the three-dimensional (3D) topography of the Moho beneath the Gofa Province Basins depicts a domal geometry. This feature extends to the east up to the western margin of the southern segment of the Main Ethiopian Rift, whereas it appears to coincides in the north with the Goba-Bonga lineament at latitude 7º 20' N. The results of the Moho depth estimates from the 2D radially-averaged power spectrum analysis are consistent with the Moho depths estimated from the seismic studies of Dugda et al. (2005) and those from the Ethiopian Afar Geophysical Lithospheric Experiment (EAGLE; Maguire et al., 2006; Keranen et al., 2009). The root mean squared error of the spectrally analyzed Moho depths with respect to the corresponding seismic Moho depths estimates (Dugda et al., 2005; Keranen et al., 2009) were calculated to be 1.6885.

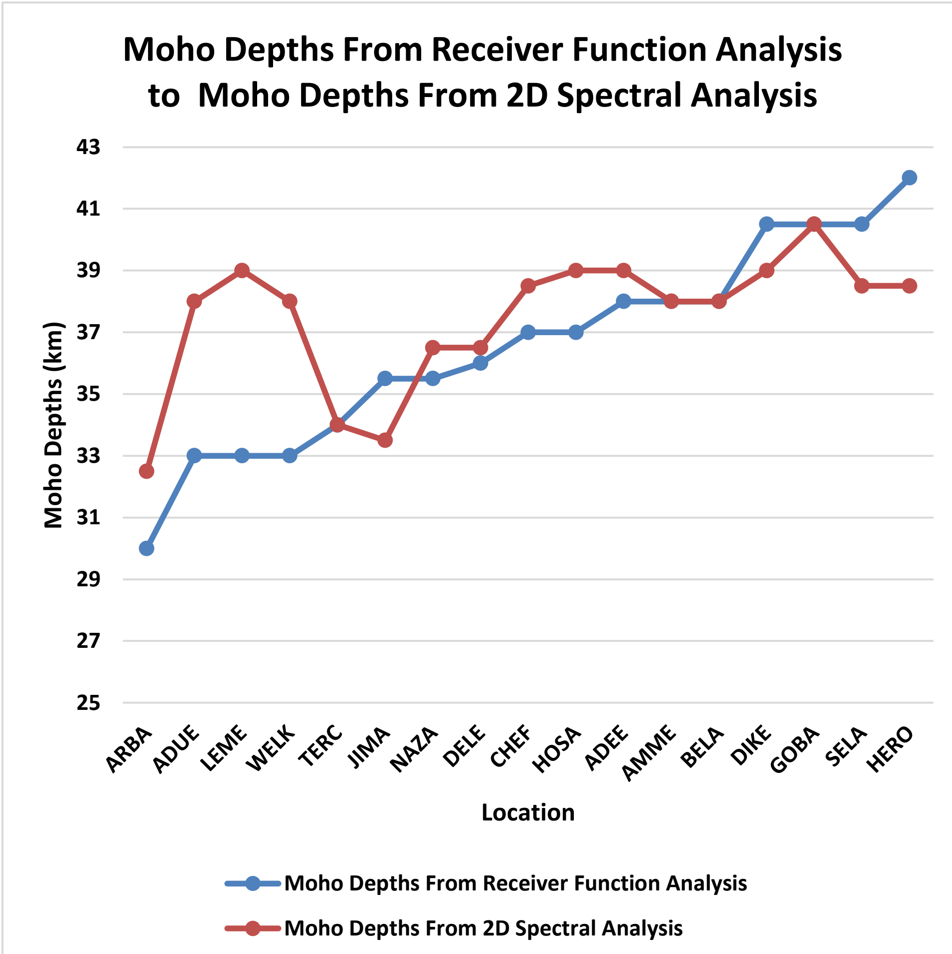

Figure 10. A chart showing a contrast between Moho depths values that are obtained from receiver function analysis to Moho depths values that are obtained from 2D spectral analysis. The root means squared error of the two data sets is calculated to be1.6885. The Moho depths results that are found from the receiver function analysis are taken from Dugda et al., (2005) and Keranen et al., (2009).

The Lithospheric Asthenospheric Boundary (LAB) depths have also been calculated from the Two-dimensional (2D) radially-averaged power spectral analysis. In so doing, only the wavenumber values (0.00773-0.046377 cyc/k-unit) that were considered as the best representatives of the deeper source were used to estimate the depths. Results show that the average lithospheric thickness of southern Ethiopia is about 105.54 km. In addition, the LAB profile indicates lithospheric flexures in two locations. The most pronounced concave downward lithospheric flexure is observed in the central part of southern Ethiopia in which there is a broadly distributed rift deformation zone on the surface. The other moderate thinning of lithosphere is observed in the Somalian plateau, which is east of the BRZ. The convex upward flexure of the lithosphere in the central part of the BRZ assumes the same geometry with the Moho surface that shows a significantly arched architecture (Figure 11).

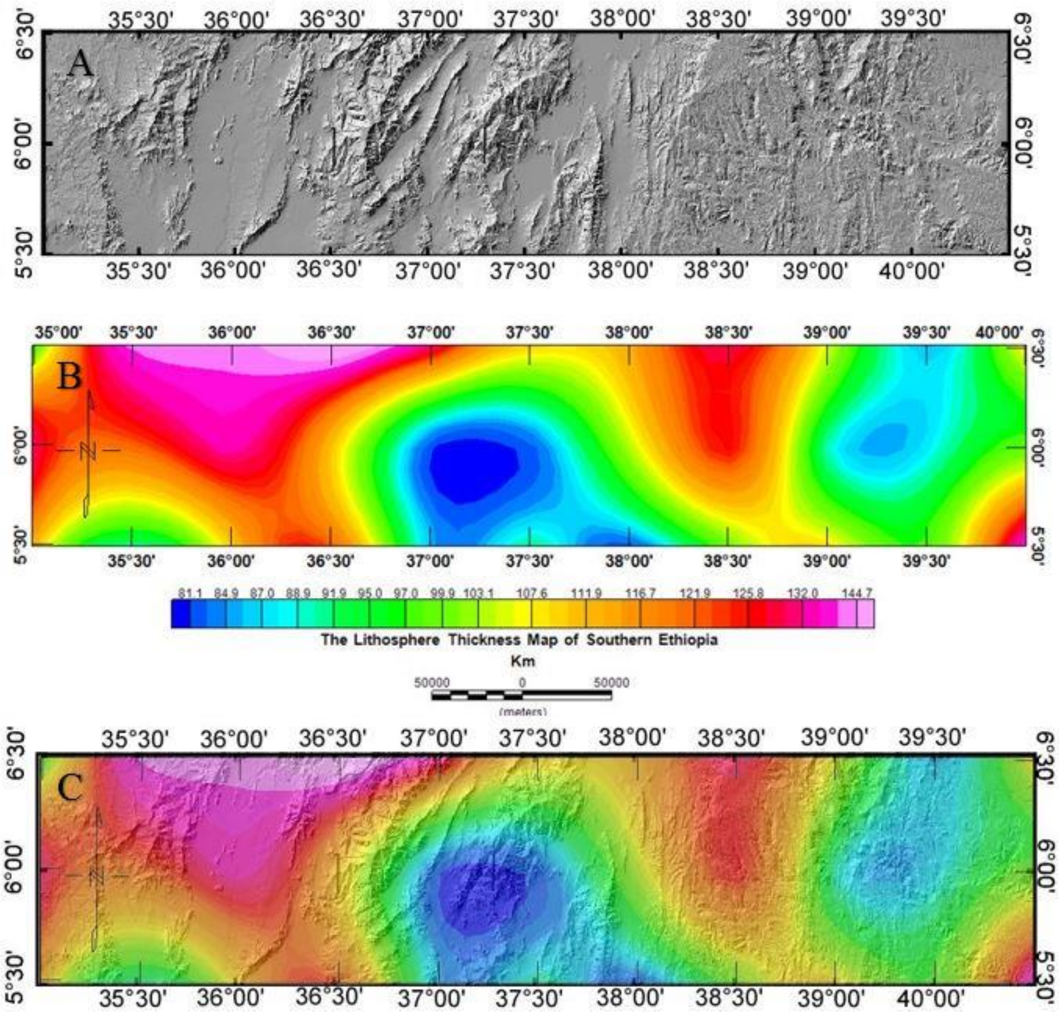

Figure 11. (A) The SRTM-DEM map of the Gofa Province Zone and its surrounding. (B) Map showing the Lithosphere Asthenosphere Boundary (LAB) of southern Ethiopia. In average, the thickness of the lithosphere is about 105.54 km. The central part of the LAB shows a pronounced convex upward architecture with a lithospheric thickness of 80 km. The geometry of the LAB in this region is similar with the Moho surface, which shows a considerable arching beneath the BRZ. (C). Figure 11 B superimposed onto Figure A.

IV.II. Results from the Two-dimensional (2D) Forward Models

One of the 2D forward models that captures the 2D gravity anomaly of 6.15º N along 33.5-40ºE transect shows an elevated Moho profile that depicts a regional arching shape in which the shallowest depth, reaching 27 km, is right underneath the Gofa Province. (Figure 9 B). The other two forward models have been constructed from the same 2D gravity anomaly map at 5º and 8ºN latitude along 35º-40ºE Longitude transects. The models generally show average crustal thickness (36 – 43 km) beneath the Omo, the SMER and the Ethiopian and Somalian plateaus. (Figure 9 A and C). The 2D forward models are consistent with the Moho map.

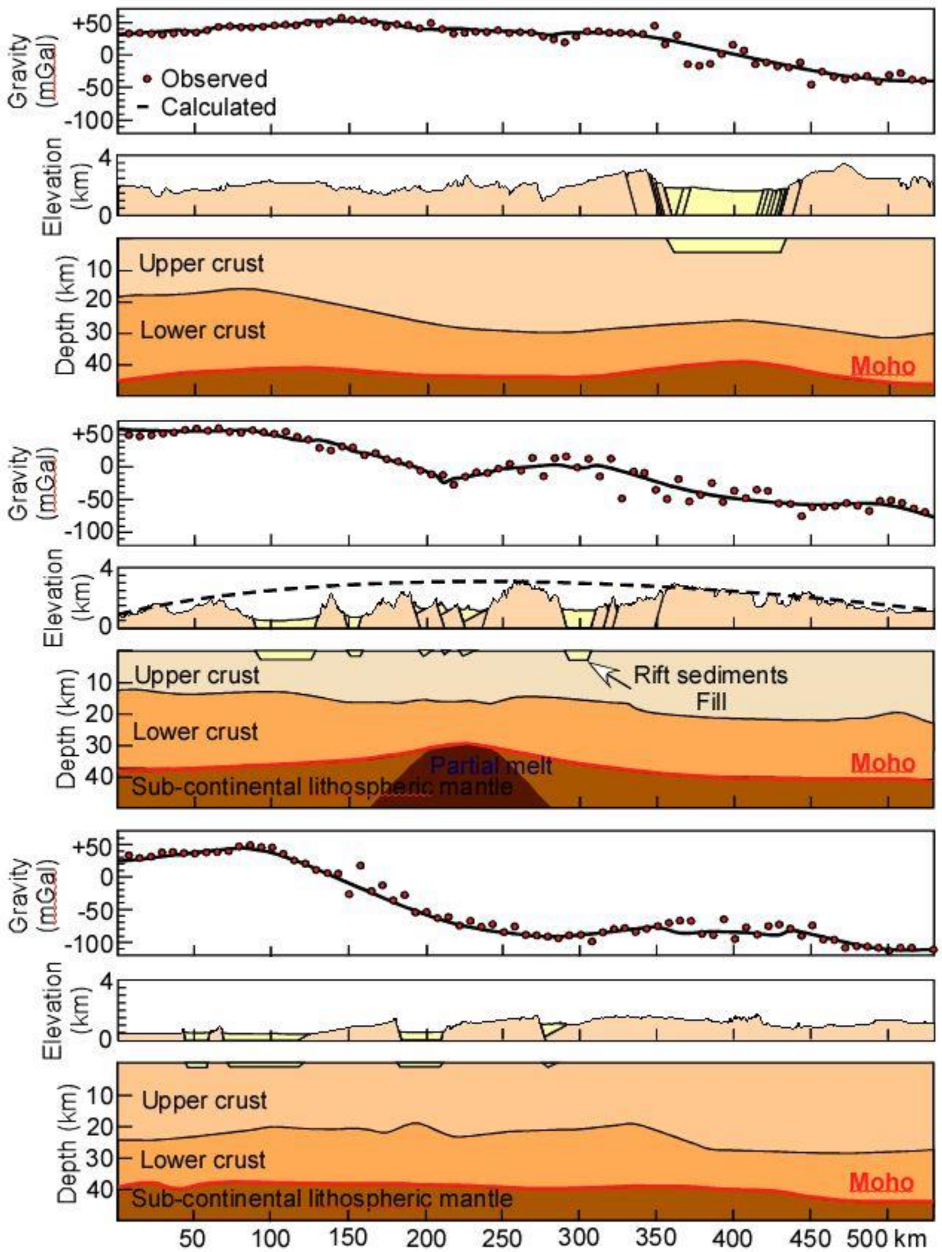

Figure 12. Cross sections of the 2D forward models constructed from WGM2012 satellite gravity data. They yellow, tan, orange and brown colors represent the sediment fills, the upper crust, the lower crust, and the sub-continental lithospheric mantle, respectively. All the profiles run from 35'E-40°E. (A) 2D forward gravity model showing the crustal scale cross section at latitude 5ºN, which shows an average continental crustal thickness of 35-40 km within an architecture of a narrow rift on the surface. (B) 2D forward gravity model at 6º 15'N. The model shows a pronounced arching of the sub-continental lithospheric mantle seating beneath the Gofa Province Basins, which is associated with the upwelling mantle plume beneath it. A similar result has been found from the 2D spectral analysis of the WGM2012 analysis, which is indicative of an extensional tectonics setting that had developed unstable topography that later on collapsed. (C) Map showing a 2D forward model of southern Ethiopia at 8°N. The model represents the SMER section in which the Moho boundary becomes deeper beneath the Somalian and Ethiopian plateaus while it is slightly elevated beneath the BRZ. The extent of the profile is as presented in Figure 7.

CHAPTER V

DISCUSSION

The analysis of gravity data and the estimation of Moho depths suggest that the central and the northern limits of the BRZ are characterized by a thin continental crust and by a domed sub-continental lithospheric mantle. The western and eastern sides of the BRZ show an average crustal thickness with some exceptions. Such heterogeneous crustal thinning is apparent within a framework in which most of the rift escarpments of the BRZ are steeply dipping. These escarpments are made of exhumed Precambrian rocks and flood basalts. The flood basalts that cover most areas of the southwestern Ethiopia display mantle plume signatures, which indicate the possible presence of mantle dynamics beneath south Ethiopia. The localization of the broad zone of BRZ's deformation at a place in which the Northern and the Eastern Branches of the EARS interacts within the Ethiopian and Kenyan domes further suggest the presence of mantle-related dynamics governing the BRZ and its immediate surrounding.

The topography of EARS, including the Northern Branch of the EARS is attributed to the upwelling of a mantle plume (Ebinger and Sleep, 1998; Rogers et al., 2000; Moucha and Forte, 2011; Saria et al., 2014; Ebinger et al., 2000). However, there have been competing ideas regarding the mantle plumes dynamics and sources. According to Ebinger and Sleep (1998), there is a single mantle plume under the stationary African plate with lateral flow and ponding. On the other hand, Rogers et al., (2000) have argued for the presence of two distinct mantle plumes: the Afar (under the Northwestern Ethiopian Plateau) and the Kenya (under the Lake Plateau Region) mantle plumes. Moucha and Forte (2011) suggest that the dynamic topography of the EARS is because of the northward movement of the African plate over the upwelling African super-plume. Thus, the BRZ may have formed by the dynamics of mantle plumes in the Northern Branch of the EARS.

V.I. Possible Deeper Sources of the Elevated Moho beneath the BRZ

Many models have been proposed to explain the source of the deeper mantle processes that might have resulted in the formation of wide rifts within heterogeneously thinned crust. The most popular of those models are the uprising of a mantle plume, detachment of a flat subducted slab, and sub-continental lithospheric mantle delamination (Fritz et al., 1996; Rey, P., 2001; Arca et al., 2010).

The BRZ has developed within 870-500 Ma old Precambrian basement (Tsige and Abdelsalam, 2005; Abdelsalam et al., 2008) that is considered as one of the fossil subduction regimes of the Pan-African Orogeny (Stern, 1994). And because there has not been an ongoing compressional stress after the Pan-African orogeny, the Neoproterozoic basement is too old to trigger mantle dynamics through the process of sub-continental lithospheric delamination. Therefore, the gravitational collapsed structures, which are initiated and developed through mantle dynamics, are not caused by sub-continental lithospheric delamination. Similarly, if there had been any flat subducted slabs during the Neoproterozoic Pan-African orogeny, those slabs are considered too old to cause any mantle related dynamics that would result in gravitationally collapse structures of the BRZ in the Miocene.

By the process of elimination, the results of this study support the uprising of a mantle plume as the cause for the formation of the BRZ. We suggest that the doming of the subcontinental lithospheric mantle and the topography of the Gofa Province, within the BRZ, are the result of mantle dynamics. Previous studies support our conclusions in that shear wave splitting, seismic body and surface wave tomography studies that have been conducted suggest the presence of two distinct mantle plumes in Afar and Kenya or southern Ethiopia (Gao et al., 2010; Steven Gao.(unpublished), Missouri Science and Technology; Figure 12 and 13).

We also suggest that the upwelling and lateral movement of the mantle plume induced extension and uplift in the BRZ. The uplift was then followed by the gravitational collapse of the region, which was mostly accommodated in the Gofa Province. The gravitational collapse of the Gofa Province Basins took place along the NW trending Mesozoic Structures and the NE trending Cenozoic Structures by forming a certain semi-circular geometry (Figure 4). The E-W directed tensile stress in southern Ethiopia may have a limited effect on the formation of the BRZ (Figure 10). The findings of this study suggest that the propagating and migrating models for the formation of the BRZ (Cerling and Powers, 1977; Moore and Davidson, 1978; WoldeGabriel and Aronson, 1987; Ebinger et al., 2000; Bonini et al., 2005; Philippon et al., 2014) need to be revised to take into account the contribution of mantle flow beneath the region.

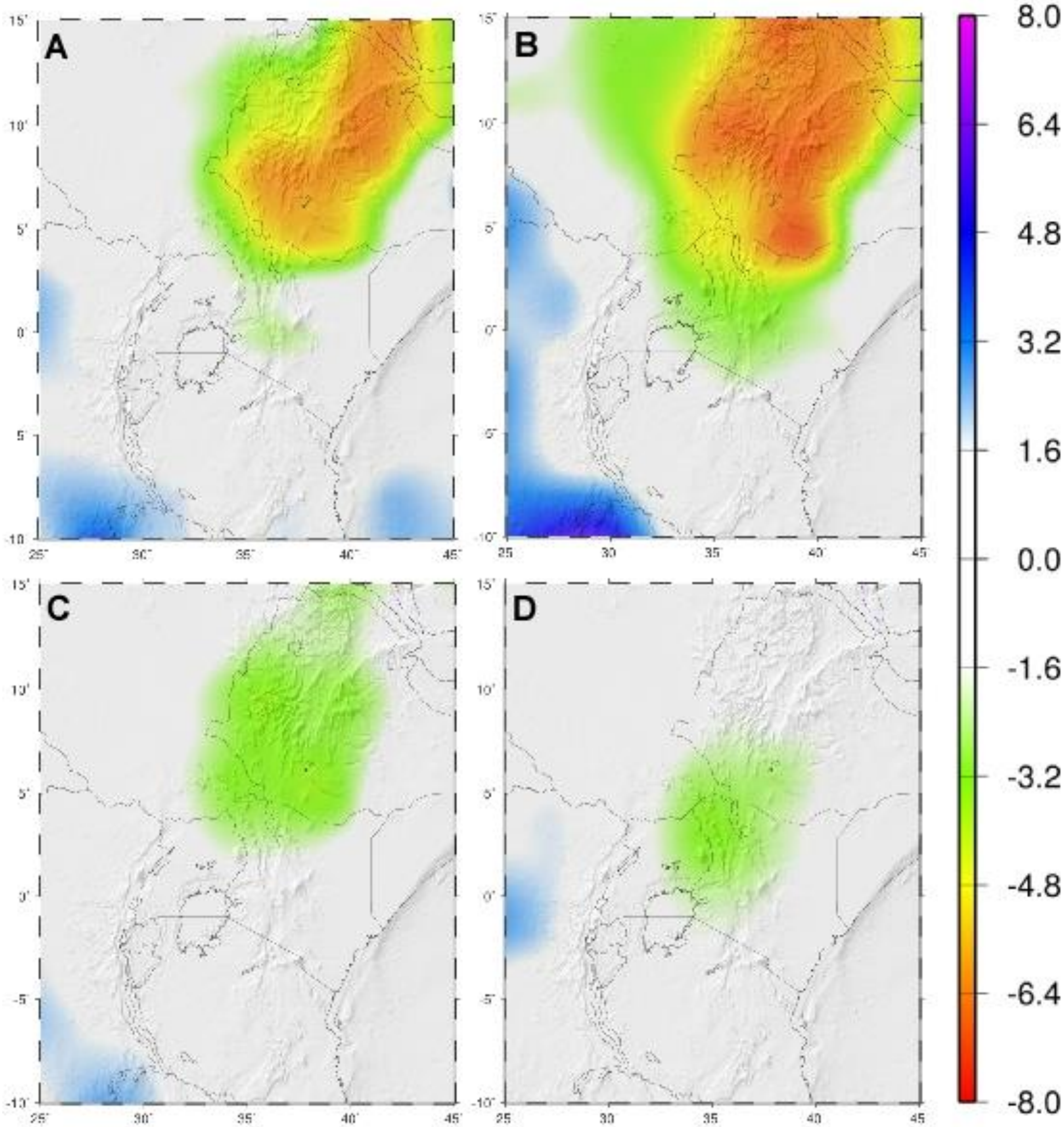

Figure 13. Map showing seismic tomography slices from the Primary Earth Reference Model (PREM). The slices from A-D, 0-325km, represent the presence of mantle plume related dynamics beneath the Main Ethiopian Rift and the Kenyan Rift (A) a tomographic slice showing the shear wave velocity of the upper lithosphere (0-100 km). The BRZ and its immediate surrounding display 6-8% slower shear wave velocity than what is normally expected. (B) Map showing a tomographic slice of 100-175 km. A broad, 6-8% lower shear wave velocity is aligned along the NE direction seating beneath the Kenyan and the Main Ethiopian rifts. This slice shows a low shear wave velocity that covers a larger surface area from the other tomographic slices. (C) Map showing a tomographic slice of 175-250 km. A localized 1.6-3.2% slower shear wave velocity region beneath the Kenyan and the Southern Main Ethiopian Rift. (D) A deeper slice showing more restricted lower shear wave velocity, 1.6-3.2%, region beneath the overlap region of the Eastern and the Northern Branches of the East African Rift System.

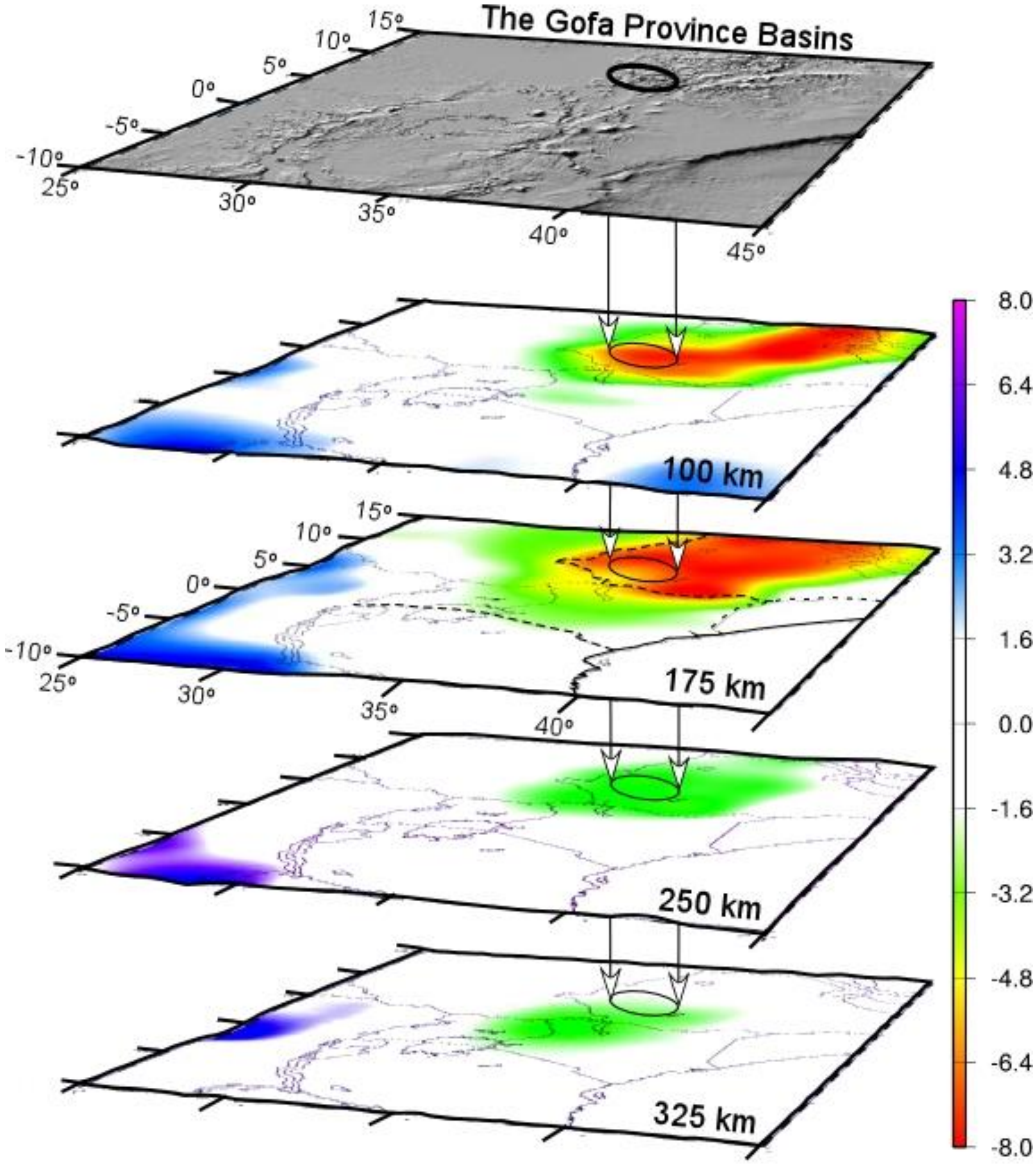

Figure 14. Map showing shear wave topographic slices. The slices show how a mantle plume related lower shear wave velocity originates and migrates in the NE direction. It started out at about 325 km at depth, and it begins to upwell and spread starting from the upper part of the asthenosphere and migrates upward all the way to the lithosphere in the NE.

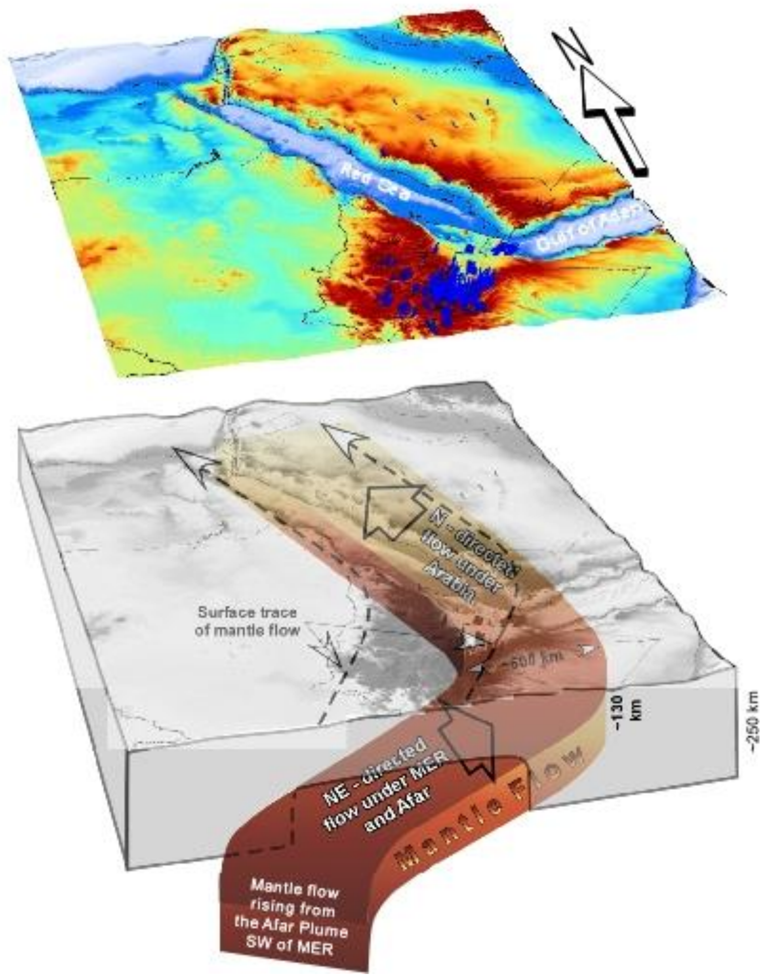

Figure 15. A conceptual model that shows the flow of a mantle plume along the MER and the eastern side of the Red Sea, which has originated beneath southern Ethiopia. Based on the seismic tomography, 2D forward models, and 2D spectral analyses results, we propose that a mantle plume originates at >325 km depth beneath the BRZ. We further suggest that there is a pronounced mantle plume influence beneath the Gofa Province Basins due to a significant arching of the Moho and Lithosphere-Asthenosphere boundaries. In addition, the arching of these discontinuities had helped the Gofa Province Basins to develop an unstable topography, which was gravitationally viable to collapse. (Figure 9 A, B-Figure 12).

We suggest that the propagation and migration of the SMER and Kenyan Rift occurred in part because of the uplift, collapse, and extension of a weakened lithosphere. Polyphase oblique rifting caused by rotation of Somalia plate (Boccaletti et al., 1998; Corti, 2009 Bonini et al., 2005) and interaction with Precambrian fabrics occurred concurrent with the vertical tectonics caused by mantle flow (Figure 13). This study suggests that mantle flow is important for the formation of a wide rift within a narrow rift system as in the case of the EARS and may also be applicable to other widening rift systems.

CHAPTER VI

CONCLUSION

The BRZ is a diffused 300 km wide rift in southern Ethiopia with surface features that resemble a Basin-and-Range type topography. This study uses gravity and structural data to understand the mechanism through which the SMER, a 48-64 km narrow rift transitioned into a 300 km wide BRZ. The 2D spectral analysis of the WGM-2012 gravity data and the 2D gravity forward model show that the BRZ has a Moho depth of about 27 km in the Gofa Province. The depths to the Moho surface radially increases away from the Gofa Province in which the deepest Moho reaches up to 43.5 km beneath the Ethiopian and Somalian Plateaus.

The dynamic topography and the sub-continental lithospheric mantle structures of the BRZ (particularly the Gofa Province) are indicative of successive uplifting episodes that resulted in unstable topography that later gravitationally collapsed.

The unstable dynamic topography of the BRZ resulted from mantle upwelling or mantle lateral flow from a deep asthenospheric source. Mantle flow may have originated from a mantle plume in the asthenosphere underneath southern Ethiopia (Gao et al., 2010). This study suggests that mantle flow is important for the formation of a wide rift within a narrow rift system in the case of the EARS and may be applicable to other rifting systems.

REFERENCES

Abdelsalam, M. G., Tsige, L., Yihunie, T., & Hussien, B. (2008). Terrane rotation during the East African Orogeny: evidence from the Bulbul Shear Zone, south Ethiopia. Gondwana Research, 14(3), 497-508.

Abebe, B., Acocella, V., Korme, T., & Ayalew, D. (2007). Quaternary faulting and volcanism in the Main Ethiopian Rift. *Journal of African Earth Sciences*, *48*(2), 115-124.

Allen, P.A., and Allen, J.R., 2005, Basin Analysis, 2nd edition: Boston, Blackwell Science.

Arca, M. S., Kapp, P., & Johnson, R. A. (2010). Cenozoic crustal extension in southeastern Arizona and implications for models of core-complex development. Tectonophysics, 488(1), 174-190.

Armitage, J. J., & Allen, P. A. (2010). Cratonic basins and the long-term subsidence history of continental interiors. *Journal of the Geological Society*, *167*(1), 61-70.

Boccaletti, M., Bonini, M., Mazzuoli, R., Abebe, B., Piccardi, L., & Tortorici, L. (1998). Quaternary oblique extensional tectonics in the Ethiopian Rift (Horn of Africa). Tectonophysics, 287(1), 97-116.

Bonini, M., Corti, G., Innocenti, F., Manetti, P., Mazzarini, F., Abebe, T., & Pecskay, Z. (2005). Evolution of the Main Ethiopian Rift in the frame of Afar and Kenya rifts propagation. Tectonics, 24(1).

Bonvalot, S., Balmino, G., Briais, A., Kuhn, M., Peyrefitte, A., & Vales, N. (2012). World Gravity Map, 1: 50000000 map/Eds. BGI-CGMW-CNES-IRD. Paris, 2012. http://bgi. obs-mip. fr/activities/Projects/world_gravity_map_ wgm.

Bridges, D. L., Mickus, K., Gao, S. S., Abdelsalam, M. G., & Alemu, A. (2012). Magnetic stripes of a transitional continental rift in Afar. *Geology*, *40*(3), 203-206.

Brun, J. P., & Gutscher, M. A. (1992). Deep crustal structure of the Rhine Graben from DEKORP-ECORS seismic reflection data: a summary. *Tectonophysics*, *208*(1), 139-147.

Buck, W.R., 1991, Modes of continental lithospheric extension: Journal Of Geophysical Research-Solid Earth, v. 96, no. B12, p. 20161–20178.

Cerling, T.E., and Powers, D.W., 1977, Paleorifting between the Gregory and Ethiopian Rifts: Geology, v. 5, no. 7, p. 441, doi: 10.1130/0091-7613(1977)5<441:PBTGAE>2.0.CO;2.

Chorowicz, J., 2005, The East African rift system: Journal Of African Earth Sciences, v. 43, no. 1-3, p. 379–410.

Chu, D., and Gordon, R., 1999, Evidence for motion between Nubia and Somalia along the southwest Indian ridge: Nature, v. 398, no. 6722, p. 64–67.

Corti, G. (2009). Continental rift evolution: from rift initiation to incipient break-up in the Main Ethiopian Rift, East Africa. Earth-Science Reviews, 96(1), 1-53.

Dugda, M. T., Nyblade, A. A., Julia, J., Langston, C. A., Ammon, C. J., & Simiyu, S. (2005). Crustal structure in Ethiopia and Kenya from receiver function analysis: implications for rift development in eastern Africa. *Journal of Geophysical Research: Solid Earth (1978–2012)*, *110*(B1).

Dunkelman, T.J., Karson, J.A., and Rosendahl, B.R., 1988, Structural style of the Turkana Rift, Kenya: Geology, v. 16, no. 3, p. 258, doi: 10.1130/0091-7613(1988)016<0258:SSOTTR>2.3.CO;2.

Ebinger, C., 1989, Tectonic Development Of The Western Branch Of The East-African Rift System: Geological Society Of America Bulletin, v. 101, no. 7, p. 885–903.

Ebinger, C.J., and Casey, M., 2001, Continental breakup in magmatic provinces: An Ethiopian example: Geology, v. 29, no. 6, p. 527–530.

Ebinger, C. J., Yemane, T., Harding, D. J., Tesfaye, S., Kelley, S., & Rex, D. C. (2000). Rift deflection, migration, and propagation: linkage of the Ethiopian and Eastern rifts, Africa. Geological Society of America Bulletin, 112(2), 163-176.

Ebinger, C. J., & Sleep, N. H. (1998). Cenozoic magmatism throughout east Africa resulting from impact of a single plume. *Nature*, *395*(6704), 788-791.

Ebinger, C. J., Yemane, T., Woldegabriel, G., Aronson, J. L., & Walter, R. C. (1993). Late Eocene–Recent volcanism and faulting in the southern main Ethiopian rift. Journal of the Geological Society, 150(1), 99-108.

Fritz, H., Wallbrecher, E., Khudeir, A. A., El Ela, F. A., & Dallmeyer, D. R. (1996). Formation of Neoproterozoic metamorphic complex during oblique convergence (Eastern Desert, Egypt). Journal of African Earth Sciences, 23(3), 311-329.

Gajewski, D., Schulte, A., Riaroh, D., and Thybo, H., 1994, Deep seismic sounding in the Turkana depression, northern Kenya rift: Tectonophysics, v. 236, no. 1, p. 165–178.

Gao, S. S., Liu, K. H., & Abdelsalam, M. G. (2010). Seismic anisotropy beneath the Afar Depression and adjacent areas: Implications for mantle flow. Journal of Geophysical Research: Solid Earth (1978–2012), 115(B12).

Goldsworthy, M., Jackson, J., & Haines, J. (2002). The continuity of active fault systems in Greece. *Geophysical Journal International*, *148*(3), 596-618.

Grand, S. P. (2002). Mantle shear–wave tomography and the fate of subducted slabs. *Philosophical Transactions of the Royal Society of London A: Mathematical, Physical and Engineering Sciences*, *360*(1800), 2475-2491.

Keranen, K. M., Klemperer, S. L., Julia, J., Lawrence, J. F., & Nyblade, A. A. (2009). Low lower crustal velocity across Ethiopia: Is the Main Ethiopian Rift a narrow rift in a hot craton?: Geochemistry, Geophysics, Geosystems, 10(5).

Kinabo, B.D., Atekwana, E.A., Hogan, J.P., Modisi, M.P., Wheaton, D.D., and Kampunzu, A.B., 2007, Early structural development of the Okavango rift zone, NW Botswana: Journal Of African Earth Sciences, v. 48, no. 2-3, p. 125–136, doi: 10.1016/j.jafrearsci.2007.02.005.

Levitte, D., Columba, J., And Mohr, P., 1974, Reconnaissance Geology of the Amaro Horst, Southern Ethiopian Rift: Geological Society Of America Bulletin, v. 85, no. 3, p. 417, doi: 10.1130/0016-7606(1974)85<417:RGOTAH>2.0.CO;2.

Lister, G. S., & Davis, G. A. (1989). The origin of metamorphic core complexes and detachment faults formed during Tertiary continental extension in the northern Colorado River region, USA. Journal of Structural Geology, 11(1), 65-94.

Maguire, P. K. H., Keller, G. R., Klemperer, S. L., Mackenzie, G. D., Keranen, K., Harder, S., ... & Amha, M. (2006). Crustal structure of the northern Main Ethiopian Rift from the EAGLE controlled-source survey; a snapshot of incipient lithospheric break-up. Special publication-geological society of London, 259, 269

Mengesha, T., Tadiwos, C., *and* H. Workineh *(*1996*)*, Geological map of Ethiopia, 2nd ed., Bulletin of the Ethiopian Institute of Geological Survey, 3*, scale 1:2.000.000, 1 sheet. OCLC: 46451457, Addis Abeba.*

Moucha, R., & Forte, A. M. (2011). Changes in African topography driven by mantle convection. *Nature Geoscience*, *4*(10), 707-712.

Moore, J. M., & Davidson, A. (1978). Rift structure in southern Ethiopia. Tectonophysics, 46(1), 159-173.

Morley, C.K., Wescott, W.A., Stone, D.M., Harper, R.M., Wigger, S.T., and Karanja, F.M., 1992, Tectonic evolution of the northern Kenyan Rift: Journal Of The Geological Society, v. 149, no. 3, p. 333–348.

Pancha, A., Anderson, J. G., & Kreemer, C. (2006). Comparison of seismic and geodetic scalar moment rates across the Basin and Range Province. *Bulletin of the Seismological Society of America*, *96*(1), 11-32.

Pavlis, N. K., Holmes, S. A., Kenyon, S. C., & Factor, J. K. (2012). The development and evaluation of the Earth Gravitational Model 2008 (EGM2008). Journal of Geophysical Research: Solid Earth (1978–2012), 117(B4).Pancha, A., Anderson, J.G., and Kreemer, C., 2006, Comparison of seismic and geodetic scalar moment rates across the Basin and Range province: Bulletin of the Seismological Society of America, v. 96, no. 1, p. 11–32.

Philippon, M., Corti, G., Sani, F., Bonini, M., Balestrieri, M. L., Molin, P., ... & Cloetingh, S. (2014). Evolution, distribution, and characteristics of rifting in southern Ethiopia. Tectonics, 33(4), 485-508.

Pik, R., Marty, B., Carignan, J., Yirgu, G., & Ayalew, T. (2008). Timing of East African Rift development in southern Ethiopia: Implication for mantle plume activity and evolution of topography. *Geology*, *36*(2), 167-170

Pik, R., Marty, B., & Hilton, D. R. (2006). How many mantle plumes in Africa? The geochemical point of view. *Chemical Geology*, *226*(3), 100-114..

Rey, P. (2001). From lithospheric thickening and divergent collapse to active continental rifting. Geological Society, London, Special Publications, 184(1), 77-88.

Rogers, N., Macdonald, R., Fitton, J. G., George, R., Smith, M., & Barreiro, B. (2000). Two mantle plumes beneath the East African rift system: Sr, Nd and Pb isotope evidence from Kenya Rift basalts. *Earth and Planetary Science Letters*, *176*(3), 387-400.

Saria, E., Calais, E., Stamps, D. S., Delvaux, D., & Hartnady, C. J. H. (2014). Present-day kinematics of the East African Rift. *Journal of Geophysical Research: Solid Earth, 119*(4), 3584-3600.Schulte-Pelkum, V., Biasi, G., Sheehan, A., and Jones, C., 2011, Differential motion between upper crust and lithospheric mantle in the central Basin and Range: Nature Geoscience, v. 4, p. 619–623, doi: 10.1038/NGEO01229.

Stamps, D.S., Calais, E., Saria, E., Hartnady, C., Nocquet, J.-M., Ebinger, C.J., and Fernandes, R.M., 2008, A kinematic model for the east African rift: Geophysical Research Letters, v. 35, no. 5, p. L05304, doi: 10.1029/2007GL032781.

Schulte-Pelkum, V., Biasi, G., Sheehan, A., & Jones, C. (2011). Differential motion between upper crust and lithospheric mantle in the central Basin and Range. *Nature Geoscience*, *4*(9), 619-623.

Stern, R. J. (1994). Arc-assembly and continental collision in the Neoproterozoic African orogen: implications for the consolidation of Gondwanaland. *Annual Review of Earth and Planetary Sciences*, *22*, 319-351.

Tselentis, G. A., Drakopoulos, J., & Dimitriadis, K. (1988). A spectral approach to Moho depths estimation from gravity measurements in Epirus (NW Greece). Journal of Physics of the Earth, 36(6), 255-266.

Tsige, L., & Abdelsalam, M. G. (2005). Neoproterozoic–Early Paleozoic gravitational tectonic collapse in the southern part of the Arabian-Nubian Shield: the Bulbul Belt of southern Ethiopia. Precambrian Research, 138(3), 297-318.

Vétel, W., and Le Gall, B., 2006, Dynamics of prolonged continental extension in magmatic rifts: the Turkana Rift case study, in Yirgu, G., Ebinger, C.J., and Maguire, P. eds., The Afar Volcanic Province within the East African Rift System, Geological Society, London, p. 209– 233.

W-Gabriel, G., and Aronson, J.L., 1987, Chow Bahir rift: A “failed” rift in southern Ethiopia: Geology, v. 15, no. 5, p. 430, doi: 10.1130/0091-7613(1987)15<430:CBRAFR>2.0.CO;2.

Wells, M.L., and Hoisch, T.D., 2008, The role of mantle delamination in widespread Late Cretaceous extension and magmatism in the Cordilleran orogen, western United States: Geological Society Of America Bulletin, v. 120, no. 5-6, p. 515–530.

Wernicke, B., 1981, Low-angle normal faults in the Basin and Range province: Nappe tectonics in an extending orogen: Nature, v. 291, no. 5817, p. 645–648.

Wernicke, B., Friedrich, A.M., Niemi, N.A., Bennett, R.A., and Davis, J.L., 2000, Dynamics of plate boundary fault systems from Basin and Range Geodetic Network (BARGEN) and geologic data: GSA Today, v. 10, no. 11, p. 1–7.

Zonenshain, L. P., & Savostin, L. A. (1981). Geodynamics of the Baikal rift zone and plate tectonics of Asia. *Tectonophysics*, *76*(1), 1-45.

VITA

LUELSEGED MENGESHA EMISHAW

Candidate for the Degree of

Master of Science

Thesis: EVOLUTION OF THE BROADLY RIFTED ZONE IN SOUTHERN ETHIOPIA THROUGH GRAVITATIONAL COLLAPSE OF DYNAMIC TOPOGRAPHY

Major Field: Geology

Biographical:

Education:

Completed the requirements for the Master of Science in Geology at Oklahoma State University, Stillwater, Oklahoma in December 2015.

Completed the requirements for the Bachelor of Science in Geology at Addis Ababa University, Addis Ababa, Ethiopia in July 2012.

Experience:

Thani Maqsam Ltd (Subsidiary of Anglo Gold Ashanti and the UAE): 11/02/2012-10/01/13

- Discriminating gold fertile tectonics habitats using geochemical pathfinder elements
- Geological mapping, Heli-assisted grab sampling, core logging and data entry

Graduate Teaching Assistant

- Taught three lab courses: physical geology, historical geology, and geology and human affairs

Publications

- Four abstracts

Relevant Coursework

- Advanced Structural Geology, Gravity and Magnetics, Signal Processing and Remote sensing, Economic Geology, Plate Tectonics, Volcanology, Research Methods

Software Experience

- ENVI, ArcGIS, Oasis Montaj, Adobe Illustrator, SPSS, Matlab, R, Office

Professional Memberships:

- GSA, SEG, Tectonic Research Group, YES network